Facile one-pot preparation of calcite mesoporous carrier for sustained and targeted drug release for cancer cells

Article *in* Chemical Communications · September 2012

DOI: 10.1039/c2cc35103j · Source: PubMed

9 authors, including:

Yuming Guo
Henan Normal University
50 PUBLICATIONS **604** CITATIONS
SEE PROFILE

Kui Wang
Henan Normal University
41 PUBLICATIONS **486** CITATIONS
SEE PROFILE

Kai Jiang
Henan Normal University
118 PUBLICATIONS **1,394** CITATIONS
SEE PROFILE

ChemComm

Cite this: *Chem. Commun.*, 2012, **48**, 10636–10638

www.rsc.org/chemcomm

COMMUNICATION

Facile one-pot preparation of calcite mesoporous carrier for sustained and targeted drug release for cancer cells†

Yuming Guo,* Jie Zhang, Lili Jiang, Xiaoman Shi, Lin Yang,* Qilong Fang, Hui Fang, Kui Wang and Kai Jiang

Received 17th July 2012, Accepted 5th September 2012
DOI: 10.1039/c2cc35103j

Herein, mesoporous calcite/chondroitin sulfate hybrid microrods are prepared through a one-pot method. Biological assays indicate that the microrods might be used as good active targeted drug delivery carriers to treat tumor tissues with high specificity and low toxic side effects.

Currently, most chemotherapeutic drugs suffer from a lack of tumor selectivity and serious side effects. Through passive or active targeting, drug delivery systems (DDS) exhibit improved efficacy and reduced side effects.[1,2] Active targeted DDS can recognize tumor sites through the modification of targeting agents.[3,4] However, hitherto, most active targeted DDS are polymer-based carriers and their applications are seriously limited by complicated preparation and safety concerns.[5,6] Therefore, the facile preparation of biocompatible active targeted DDS has attracted considerable attention. Considering the advantages over polymers, including facile preparation and non-involvement of toxic reagents, inorganic materials might be good candidates for DDS. Several studies have reported the applications of porous SiO_2 as a DDS.[7,8] However, most of these SiO_2-based DDS are passive targeted systems and just own the lower targeting effect than the active systems.[9] Compared with SiO_2, $CaCO_3$ exhibits ideal biocompatibility and biodegradability and might be used as an ideal DDS candidate. However, so far, reports about the application of $CaCO_3$ as a DDS are rare,[10,11] especially as an active targeted DDS.

Herein, using chondroitin sulfate (CS) as the targeting agent and the morphology–directing matrix simultaneously, CS/calcite hybrid mesoporous microrods (CS–CaMRs) were successfully prepared through a facile one-pot strategy. Biological assays revealed that doxorubicin hydrochloride (DOX·HCl) could be efficiently loaded into the carrier, delivered to the target cancer cells and released in a sustained fashion to exert its anticancer effect. Furthermore, the targeted delivery and sustained release significantly enhanced the anticancer effect and decreased the toxic side effects of DOX·HCl. This suggests that the as-prepared CS–CaMRs might be used as a potential targeted DDS to treat cancer with high specificity.

A possible mechanism for the preparation of CS–CaMRs and the targeted delivery and sustained release of DOX·HCl is shown in Scheme 1. Firstly, after mixing of Ca^{2+} and CS, the Ca^{2+} accumulates around the CS through the interactions between Ca^{2+} and CS. Then, calcite/CS hybrid nanoparticles are formed after the addition of Na_2CO_3 and self-assemble into mesoporous microrods. Secondly, DOX·HCl is loaded into the microrods. Thirdly, through the specific ligand–receptor interactions between CS and CD44 receptors, the CS–CaMRs/DOX·HCl are specifically delivered and accumulate around the cancer cell. Then the CS–CaMRs/DOX·HCl could be internalized into the cancer cells through receptor-mediated endocytosis and some of the CS–CaMRs/DOX·HCl could be decomposed under the weakly acidic conditions inside the cancer cells. Finally, the internalized CS–CaMRs/DOX·HCl are decomposed and a

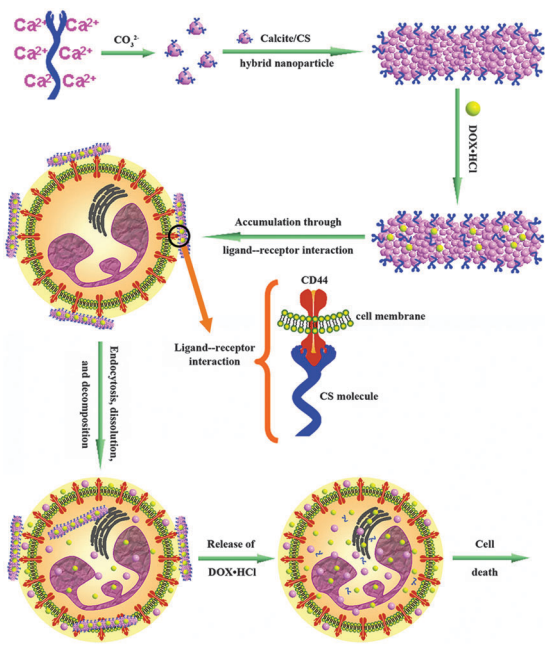

Scheme 1 Possible mechanism for the formation of CS–CaMRs in the presence of CS, the targeted delivery of CS–CaMRs/DOX·HCl and the sustained release of DOX·HCl for the treatment of HeLa cells.

College of Chemistry and Chemical Engineering, Key Laboratory of Green Chemical Media and Reactions, Ministry of Education, Henan Normal University, Xinxiang, 453007, P.R. China. E-mail: guoyuming@gmail.com, yanglin1819@163.com; Fax: +86-373-3328507; Tel: +86-373-3325058

† Electronic supplementary information (ESI) available: Experimental details and supplementary results. See DOI: 10.1039/c2cc35103j

large amount of DOX·HCl molecules are released, resulting in cell death.

The morphology of the CS–CaMRs was observed by SEM and TEM. From these results, the CS–CaMRs exhibit well-dispersed rod-like structures (Fig. 1a) and a narrow size distribution with an average diameter of 397.6 nm and length of 1.28 μm (Fig. S1a–b, ESI†). From field-emission SEM (Fig. 1a inset) and TEM images (Fig. 1b), the CS–CaMRs are composed of nanoparticles with an average size of 5.99 nm (Fig. S1c, ESI†). Moreover, the obvious space between the nanoparticles (Fig. 1a inset) indicates the presence of pores. Through multipoint Brunauer–Emmett–Teller (BET) analysis, the specific surface area (SSA) is 83.9 m^2 g^{-1} (Fig. S2, ESI†) and the average size of the pores is 25 nm, indicating the mesoporous feature of the CS–CaMRs.[12] In addition, from Fig. S3 and Fig. S4 (ESI†), the products from 0.1 wt%, 0.2%, 0.3 wt%, and 0.5 wt% CS are not microrods, but irregular aggregates. Furthermore, the control product obtained in the absence of CS is a cubic-like aggregate. This reveals the importance of CS for the formation of microrods.

By XRD analysis, the CS–CaMRs exhibit identical diffraction peaks to calcite (PDF 83-0578) (Fig. 1c). In the FT-IR measurements, compared with the spectrum of CS (Fig. 1d), in addition to the characteristic bands of calcite at 713 and 874 cm^{-1},[13] the absorption bands of –C–O, –OH, $-(SO_3)^-$, $-COO^-$, and –N–H of the CS are also detected in the CS–CaMRs, indicating the presence of CS. Furthermore, the positions and intensities of the absorption bands of these groups change to some extent, revealing the interactions between the calcite and these groups. From the TG-DSC analysis (Fig. 1e), the CS content in the CS–CaMRs is 5.26%.

The formation process of the CS–CaMRs was evaluated through time-dependent observations. From Fig. S5 (ESI†), the nanoparticles are formed when Na_2CO_3 is added and assemble into twin spheres after 10 min. After 3 h, a large amount of pseudorods are formed. After 24 h, the mesoporous microrods are formed. From Fig. S5 (ESI†), the main exposed faces of the products after 10 min and 24 h are (006) and (110) respectively, indicating the transformation of the habit faces during microrod formation. Based on the optimized models of the (110) and (006) faces (Fig. S6, ESI†), the (110) faces are neutral-charged faces and possess low surface energy. However, the (006) faces consist of Ca^{2+} and have higher surface energy. It should be the surface energy difference between (110) and (006) that drives the transformation of the habit faces and results in the formation of the microrods.

Using DOX·HCl as a model drug, the potential application of the CS–CaMRs as a targeted DDS was studied. The red autofluorescence of DOX·HCl was used to monitor the loading effect. From Fig. S7 (ESI†), the red fluorescence of CS–CaMRs/DOX·HCl indicates the efficient loading of DOX·HCl. UV-Vis spectroscopic analysis indicated that the loading content and entrapment of DOX·HCl were 5.782% and 57.82%, respectively.

Tumor tissues have a lower local pH (5–6) than normal tissues (7.4), which is an intrinsic feature of tumors[14] and can be exploited as a drug release trigger for pH-sensitive carriers. Therefore, the release experiments were performed at different pH values. Fig. 2a shows that the release efficiency under acidic conditions is much higher than under neutral conditions, which can be attributed to the pH sensitivity of the microrods. This suggests that the CS–CaMRs might be used as a good pH-sensitive DDS to release drugs into tumor tissues. Furthermore, after initial burst release within the first 24 h, DOX·HCl showed a sustained release profile over 20 days. The sustained release might yield the sustained level of DOX·HCl required to exert the anticancer effect for a much longer duration than the pure drug, thereby effectively avoiding the need for frequent administration.

It is well known that CD44 is a membrane glycoprotein that is overexpressed by cancer cells, such as HeLa cells.[15] From previous studies, CS molecules can function as ligands to specifically combine with CD44.[16] This specific interaction endows the CS–CaMRs with the targeted delivery feature for HeLa cells. From Fig. 2b–c,

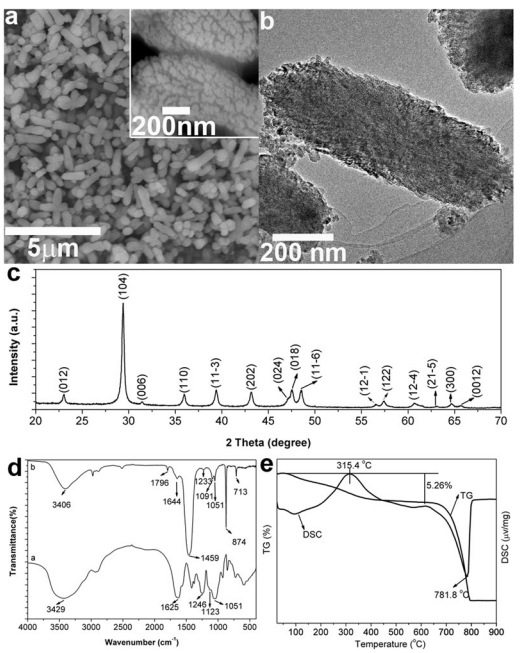

Fig. 1 (a) SEM image of the CS–CaMRs. Inset: FESEM image. (b) TEM image and (c) XRD pattern of the CS–CaMRs. (d) FT-IR spectra of the CS and the CS–CaMRs. (e) TG-DSC curves of the CS–CaMRs.

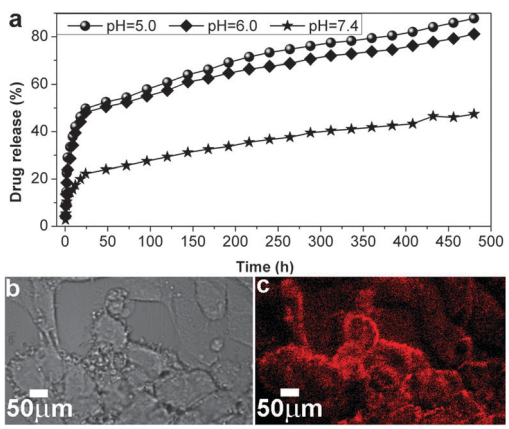

Fig. 2 (a) *In vitro* release profiles of the CS–CaMRs/DOX·HCl under different pH values. $n = 6$, each data point represents the mean ± standard deviation. (b) Light and (c) fluorescence micrographs of the HeLa cells after treatment with CS–CaMRs/DOX·HCl for 12 h.

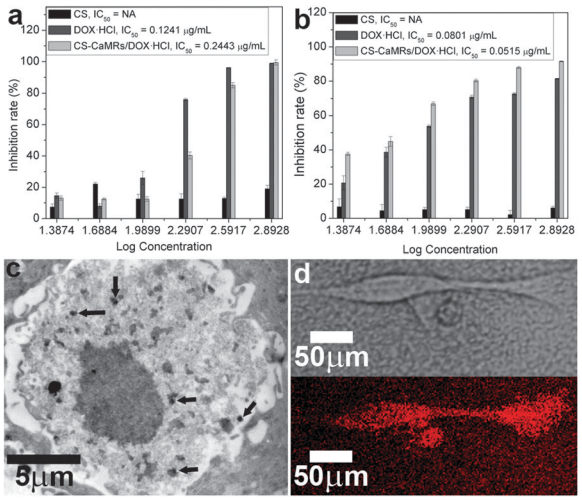

Fig. 3 (a) Cytotoxic effects of CS, free DOX·HCl, and CS–CaMRs/DOX·HCl on V79-4 and (b) HeLa cells after 120 h treatment ($n = 6$). (c) TEM image and (d) light and fluorescence micrographs of the HeLa cells after treatment with CS–CaMRs/DOX·HCl for 120 h. The calcite nanoparticles in the cells are highlighted with black arrows.

after treatment with CS–CaMRs/DOX·HCl for 12 h, the strong red fluorescence around the cell edges indicates that the CS–0CaMRs/DOX·HCl are specifically localized around the HeLa cells. However, it cannot be localized to the surface of V79-4 cells (Fig. S9, ESI†). This demonstrates the targeted delivery feature of the CS–CaMRs/DOX·HCl for HeLa cells, rather than V79-4 cells.

From the MTT assay (Fig. 3a), after treatment for 120 h, the IC_{50} of CS–CaMRs/DOX·HCl for V79-4 cells is 0.2443 μg mL^{-1}, about two times that of the free drug (0.1241 μg mL^{-1}). This reveals a significant decrease in the undesirable side effects of DOX·HCl on normal cells. From Fig. 3b, the IC_{50} of CS–CaMRs/DOX·HCl for HeLa cells is 0.0515 μg mL^{-1}, much lower than that of the free drug (0.0801 μg mL^{-1}). This indicates a significant enhancement of the desirable anticancer effect of DOX·HCl on cancer cells. For a given anticancer drug, the specificity can be expressed as the IC_{50} ratio for normal and cancer cells. The higher the ratio, the stronger the specificity.[17] Based on this idea, the specificities of the DOX·HCl and CS–CaMRs/DOX·HCl are 1.5493 and 4.7437, respectively. The specificity of DOX·HCl is significantly enhanced after loading into the CS–CaMRs (about 3.06 times that of the free drug). This indicates that CS–CaMRs can significantly enhance both the anticancer effect and the specificity.

From ICP-MS analysis, after incubation in Eagle's minimum essential medium (EMEM) medium for 120 h, the $[Ca^{2+}]$ is 85.5 mg L^{-1}, similar to the pure medium. Moreover, the incubated CS–CaMRs retain the microrod structure (Fig. S10a, ESI†), demonstrating the stability of CS-CaMRs in the EMEM medium. However, after incubation with HeLa cells, the $[Ca^{2+}]$ is 127.0 mg L^{-1}, much higher than that of the EMEM medium. Furthermore, the incubated CS–CaMRs turn into nanoparticles (Fig. S10b, ESI†), revealing the biodegradability of the CS–CaMRs in the system of HeLa cells. This can be attributed to the gradual dissolution and decomposition of the calcite in the weakly acidic environment of the HeLa cells.

In addition, after treatment with CS–CaMRs/DOX·HCl, the HeLa cells were observed by TEM. From Fig. 3c, the CS–CaMRs and the decomposed calcite nanoparticles can be found inside the cells, indicating the internalization of the CS–CaMRs and the decomposed nanoparticles into the HeLa cells by receptor-mediated endocytosis. Furthermore, the whole HeLa cell emits strong red fluorescence (Fig. 3d). This confirms the internalization of CS–CaMRs/DOX·HCl and the release of DOX·HCl, which finally results in cell death.

In summary, CS molecules can not only be used as the morphology-directing agent to prepare CS–CaMRs, but can also be used as the targeting agent to specifically interact with CD44. The CS–CaMRs can be efficiently loaded and used for targeted delivery and sustained release of anticancer drugs to treat cancer cells. This suggests that CS–CaMRs might be used as active targeted DDS to treat tumors with high specificity and low toxic side effects.

This work was financially supported by the National Science Foundation of China (21171051, 21271066), the Program for Changjiang Scholars and Innovative Research Team in University (IRT1061), the Innovation Fund for Outstanding Scholar of Henan Province (114200510004), the Henan Key Proposed Program for Basic and Frontier Research (112102210005, 112300410095) and the Key Young Teachers Project of Henan Province (2012GGJS-065) and Henan Normal University.

Notes and references

1 J. D. Byrne, T. Betancourt and L. Brannon-Peppas, *Adv. Drug Delivery Rev.*, 2008, **60**, 1615–1626.
2 X. Ma, H. Chen, L. Yang, K. Wang, Y. Guo and L. Yuan, *Angew. Chem., Int. Ed.*, 2011, **50**, 7414–7417.
3 A. P. Chapman, *Adv. Drug Delivery Rev.*, 2002, **54**, 531–545.
4 H. Otsuka, Y. Nagasaki and K. Kataoka, *Adv. Drug Delivery Rev.*, 2003, **55**, 403–419.
5 V. Gajbhiye and N. K. Jain, *Biomaterials*, 2011, **32**, 6213–6225.
6 X. Li, Y. Qian, T. Liu, X. Hu, G. Zhang, Y. You and S. Liu, *Biomaterials*, 2011, **32**, 6595–6605.
7 F. Muhammad, M. Guo, W. Qi, F. Sun, A. Wang, Y. Guo and G. Zhu, *J. Am. Chem. Soc.*, 2011, **133**, 8778–8781.
8 A. Schlossbauer, C. Dohmen, D. Schaffert, E. Wagner and T. Bein, *Angew. Chem., Int. Ed.*, 2011, **50**, 6828–6830.
9 B. P. Timko, K. Whitehead, W. Gao, D. S. Kohane, O. Farokhzad, D. Anderson and R. Langer, *Annu. Rev. Mater. Res.*, 2011, **41**, 1–20.
10 W. Wei, G.-H. Ma, G. Hu, D. Yu, T. McLeish, Z.-G. Su and Z.-Y. Shen, *J. Am. Chem. Soc.*, 2008, **130**, 15808–15810.
11 Y. Zhao, Y. Lu, Y. Hu, J.-P. Li, L. Dong, L.-N. Lin and S.-H. Yu, *Small*, 2010, **6**, 2436–2442.
12 K. S. W. Sing, D. H. Everett, R. A. W. Haul, L. Moscow, R. A. Pieroffl, J. Rouquerol and T. Siemieni-Ewska, *Pure Appl. Chem.*, 1985, **57**, 603–619.
13 G. Falini, S. Albeck, S. Weiner and L. Addadi, *Science*, 1996, **271**, 67–69.
14 M. Stubbs, P. M. J. McSheehy, J. R. Griffiths and C. L. Bashford, *Mol. Med. Today*, 2000, **6**, 15–19.
15 A. Skoudy, J. Mounier, A. Aruffo, H. Ohayon, P. Gounon, P. Sansonetti and G. Tran Van Nhieu, *Cell. Microbiol.*, 2000, **2**, 19–33.
16 M. F. Naujokas, M. Morin, M. S. Anderson, M. Peterson and J. Miller, *Cell*, 1993, **74**, 257–268.
17 P. Phatak, F. Dai, M. Butler, M. P. Nandakumar, P. L. Gutierrez, M. J. Edelman, H. Hendriks and A. M. Burger, *Clin. Cancer Res.*, 2008, **14**, 4593–4602.